

## Raman spectroscopy of the mineral rhodonite

Stuart J. Mills<sup>a,b</sup>, Ray L. Frost<sup>c</sup>, J. Theo Kloprogge<sup>c</sup> and Matt L. Weier<sup>c</sup>

<sup>a</sup> Geosciences, Museum Victoria, PO Box 666E, Melbourne, Victoria 3001, Australia.

<sup>b</sup> CSIRO Minerals, Box 312, Clayton South, Victoria 3169, Australia.

<sup>c</sup> Inorganic Materials Research Program, School of Physical and Chemical Sciences, Queensland University of Technology, GPO Box 2434, Brisbane, Queensland 4001, Australia.

This is the authors' version of a paper that was later published in:  
(2005) *Spectrochimica Acta* 62(1): pp171-175

Copyright (2005) Elsevier

### Abstract

The mineral rhodonite an orthosilicate has been characterised by Raman spectroscopy. The Raman spectra of three rhodonites from Broken Hill, Pachapaqui and Franklin were compared and found to be similar. The spectra are characterised by an intense band at around 1000 cm<sup>-1</sup> assigned to the  $\nu_1$  symmetric stretching mode and three bands at 989, 974 and 936 cm<sup>-1</sup> assigned to the  $\nu_3$  antisymmetric stretching modes. An intense band at around 667 cm<sup>-1</sup> was assigned to the  $\nu_4$  bending mode and showed additional bands exhibiting loss of degeneracy of the SiO<sub>4</sub> units. The low wavenumber region of rhodonite is complex. A strong band at 421.9 cm<sup>-1</sup> is attributed to the  $\nu_2$  bending mode. The spectra of the three rhodonite mineral samples are similar but subtle differences are observed. It is proposed that these differences depend upon the cationic substitution of Mn by Ca and/or Fe<sup>2+</sup> and Mg.

**Keywords:** rhodonite, orthosilicate, Raman spectroscopy, infrared spectroscopy

### Introduction

The mineral rhodonite ((Mn<sup>2+</sup>,Fe<sup>2+</sup>,Mg,Ca)SiO<sub>3</sub>) has been studied some time [1-3]. Indeed because the mineral is highly coloured it has been studied by UV-visible absorption spectroscopy [4-6]. The mineral is one of a group of silicates known as an orthosilicates. The mineral can be used as a form of jewellery and has a semi-precious status. The infrared spectroscopy of rhodonite has been studied [7]. However no analysis of the structure was made. Infrared spectroscopy has been used to estimate the heat capacity of minerals including rhodonite [8]. The optical absorption of rhodonite has been elucidated [9] and studies of the surface properties using glancing X-ray techniques undertaken [10-12]. To the best of the authors knowledge no Raman spectroscopic studies of rhodonite have been forthcoming.

If the assumption is made that rhodonite structure is similar to an orthosilicate and that a large cation perturbs the tetrahedral SiO<sub>4</sub> units, then an analysis of the Raman spectra of rhodonite should be able to be undertaken. Indeed a comparison

---

\* Author to whom correspondence should be addressed (r.frost@qut.edu.au)

between rhodonites from different origins made. A tetrahedral  $\text{SiO}_4$  molecule not involved in distortion should have four vibrational modes. These are the  $\nu_1$  symmetric stretching mode, the  $\nu_2$  doubly degenerate bend, the  $\nu_3$  triply degenerate antisymmetric stretching mode and the  $\nu_4$  triply degenerate bending mode. For tetrahedral  $\text{SiO}_4$  units, the  $\nu_3$  and  $\nu_4$  modes will be infrared active and the  $\nu_1$  and  $\nu_2$  modes Raman active. If a cation causes the reduction in the tetrahedral symmetry the degeneracy of the vibrational modes will be removed. Farmer reports that for a heavy cationic silicate such as  $\text{BaSiO}_4$ , the  $\nu_3$  modes occur between 880 and 940  $\text{cm}^{-1}$ ,  $\nu_4$  a doublet at 493 and 510  $\text{cm}^{-1}$ ,  $\nu_1$  is a weak band at 826  $\text{cm}^{-1}$  [13]. Tarte showed that for the olivine series there was a linear relationship between position of the  $\text{SiO}_4$  bands and the cationic radius. A similar relationship has been observed for the position of the bands and unit cell dimensions for the garnet group of minerals. In this work we report the analyses of three rhodonites of different origins and related the Raman spectra to the structure.

## **Experimental**

### **Minerals**

Samples of rhodonite were obtained from Museum Victoria. Sample m33277 originated from Broken Hill, NSW, Australia. Sample m39445 was from Pachapaqui District, Bolognesi Province, Ancash Department, Peru and sample m40106 was from Franklin, Ogdensburg, Sussex County, New Jersey, USA.

### ***Raman microprobe spectroscopy***

Samples of rhodonite were placed and orientated on the stage of an Olympus BSM microscope, equipped with 10x and 50x objective lenses, as part of a Renishaw 1000 Raman microscope system. This system also includes a monochromator, filter system and a Charge Coupled Device (CCD). Raman spectra were excited by a HeNe laser (633 nm) at a resolution of 2  $\text{cm}^{-1}$  in the range between 100 and 4000  $\text{cm}^{-1}$ . Repeated acquisition using the highest magnification was undertaken to improve the signal-to-noise ratio. Spectra were calibrated using the 520.5  $\text{cm}^{-1}$  line of a silicon wafer. In order to ensure that the correct spectra were obtained, the incident excitation radiation was scrambled. Previous studies provide an in depth account of the experimental technique [14-19]. Spectral manipulation such as baseline adjustment, smoothing and normalisation was performed using the GRAMS® software package (Galactic Industries Corporation, Salem, NH, USA).

## **Results and discussion**

The Raman spectra in the 800 to 1150  $\text{cm}^{-1}$  range of the three rhodonite samples are shown in **Figure 1**. The results of the spectral analyses are reported in **Table 1**. A strong similarity is shown in the spectral profiles of this region between all three rhodonite samples. It is apparent that the most intense band is observed at 999  $\text{cm}^{-1}$  (Broken Hill), 1000.3  $\text{cm}^{-1}$  (Pachapaqui) and 1003.0  $\text{cm}^{-1}$  (Franklin). This band is assigned to the  $\nu_1$  symmetric stretching mode of the  $\text{SiO}_4$  units. The band for zircon was reported as occurring at 974  $\text{cm}^{-1}$  [20].

Three bands are observed at around 989, 974 and 936  $\text{cm}^{-1}$  and are assigned to the three components of the  $\nu_3$  vibration. Slight variation occurs in the position of the bands between the samples. However this is well within experimental error. In the infrared spectrum of zircon three bands at 989, 1008 and 885  $\text{cm}^{-1}$  were observed [20]. A band is found in all of the spectra at around 877  $\text{cm}^{-1}$ . This band is considered to be a water librational mode which results from the replacement of  $\text{O}^{2-}$  ions by  $\text{OH}^-$  ions in the rhodonite structure [21]. Evidence for the existence of water librational bands is confirmed by the presence of OH stretching bands in the spectral region from 3000 to 4000  $\text{cm}^{-1}$ . A band is also observed at 1052  $\text{cm}^{-1}$ . The attribution of this band is not known but one possibility is that it is an OH deformation vibration.

The 600 to 800  $\text{cm}^{-1}$  region of the Raman spectra of the three rhodonites are shown in **Figure 2**. An intense Raman band is observed at 667.3  $\text{cm}^{-1}$  (Broken Hill, 667.5  $\text{cm}^{-1}$  (Pachapaqui) and 670.0  $\text{cm}^{-1}$  (Franklin). The band is sharp with bandwidths between 11.0 and 11.7  $\text{cm}^{-1}$ . Some splitting of the band is observed with a band at 680  $\text{cm}^{-1}$  observed in each spectrum. For the Pachapaqui and Franklin samples, an additional band is observed on the low wavenumber side at 659 and 664.6  $\text{cm}^{-1}$ . If the assignment of bands according to Dawson et al. [20] is followed then these bands are assigned to the  $\nu_4$  bending mode. The observation of multiple bands shows at least a partial loss of degeneracy.

The Raman spectra of the low wavenumber region are shown in **Figure 3**. For the Franklin rhodonite an intense band is observed at 421.9  $\text{cm}^{-1}$ . Other low intensity bands are observed at 455, 439, 3409, 391 and 366  $\text{cm}^{-1}$ . These bands are of  $A_{1g}$  symmetry and are polarised. Dawson et al proposed the band in this position for zircon was attributable to the  $\nu_2$  mode [20]. One probable assignment is that these bands are attributed to the  $\nu_2$  bending modes. The observation of multiple bands in this region shows the exact non-equivalence of the  $\text{SiO}_4$  tetrahedra. The observation of multiple bands shows loss of degeneracy of these tetrahedra. A second internal mode of the  $\text{SiO}_4$  tetrahedra of  $B_{2g}$  symmetry is observed at 263 and 277.5  $\text{cm}^{-1}$ . These are also  $\nu_2$  bending modes. The low wavenumber region of the Raman spectra of rhodonite is complex and consists of multiple sets of overlapping bands. Some of these bands may be due to rotatory and translational modes.

## Conclusions:

Raman spectroscopy has been used to characterise three rhodonites from different origins. The spectra of the minerals are similar but subtle differences are observed. It is proposed that these differences depend upon the cationic substitution of Mn by Ca and/or  $\text{Fe}^{2+}$  and Mg. The minerals are characterised by a set of overlapping bands centred around 1000  $\text{cm}^{-1}$  consisting of a symmetric stretching mode at 999  $\text{cm}^{-1}$  and three antisymmetric modes at 989, 974 and 936  $\text{cm}^{-1}$ . An intense band at around 667  $\text{cm}^{-1}$  was assigned to the  $\nu_4$  bending mode and showed additional bands exhibiting loss of degeneracy of the  $\text{SiO}_4$  units. The low wavenumber region of rhodonite is complex. A strong band at 421.9  $\text{cm}^{-1}$  is attributed to the  $\nu_2$  bending mode.

## **Acknowledgements**

The financial and infrastructure support of the Queensland University of Technology Inorganic Materials Research Program of the School of Physical and Chemical Sciences is gratefully acknowledged. The Australian Research Council (ARC) is thanked for funding. Museum Victoria, CSIRO Minerals and the Smithsonian Institute are thanked for the loan of the minerals. SJM wishes to thank the support of CSIRO Minerals.

## References

- [1]. F. M. Jager and H. S. Van Klooster, *J. Soc. of Glass Technol.* 3 (1919) 234.
- [2]. A. N. Lazarev and T. F. Tenisheva, *Optika i Spektroskopiya* 11 (1961) 584.
- [3]. S. V. Grum-Grzhimailo, *Zapiski Vserossiiskogo Mineralogicheskogo Obshchestva* 91 (1962) 86.
- [4]. P. G. Manning, *Can. Min.* 9 (1968) 348.
- [5]. M. Marshall and W. A. Runciman, *Am. Min.* 60 (1975) 88.
- [6]. K. Zhou, Z. Zhang, J. Yang and J. Zhang, *Huaxue Wuli Xuebao* 1 (1988) 300.
- [7]. G. Agiorgitis, *Tschemaks Mineralogische und Petrographische Mitteilungen* 13 (1969) 273.
- [8]. G. A. Narnov, *Mineral. Issled. Dal'nem Vostoke* (1977) 123.
- [9]. S. V. J. Lakshman and B. J. Reddy, *Physica* 66 (1973) 601.
- [10]. M. L. Farquhar, R. A. Wogelius, J. M. Charnock, P. Wincott, C. C. Tang, M. Newville, P. J. Eng and T. P. Trainor, *Min. Mag.* 67 (2003) 1205.
- [11]. L. A. J. Garvie and A. J. Craven, *Phys. Chem. Min.* 21 (1994) 191.
- [12]. P. E. Petit, F. Farges, M. Wilke and V. A. Sole, *J. Synchrotron Rad.* 8 (2001) 952.
- [13]. V. C. Farmer, *Mineralogical Society Monograph 4: The Infrared Spectra of Minerals*, 1974.
- [14]. R. L. Frost, M. Crane, P. A. Williams and J. T. Kloprogge, *J. Raman Spec.* 34 (2003) 214.
- [15]. R. L. Frost, P. A. Williams and W. Martens, *Min. Mag.* 67 (2003) 103.
- [16]. W. Martens, R. L. Frost and J. T. Kloprogge, *J. Raman Spec.* 34 (2003) 90.
- [17]. W. Martens, R. L. Frost, J. T. Kloprogge and P. A. Williams, *J. Raman Spec.* 34 (2003) 145.
- [18]. R. L. Frost, W. Martens, J. T. Kloprogge and P. A. Williams, *J. Raman Spec.* 33 (2002) 801.
- [19]. R. L. Frost, W. Martens, P. A. Williams and J. T. Kloprogge, *Min. Mag.* 66 (2002) 1063.
- [20]. P. Dawson, M. M. Hargreave and G. R. Wilkinson, *J. Physics C.* 4 (1971) 240.
- [21]. R. W. T. Wilkins and W. Sabine, *Am. Min.* 58 (1973) 508.

<b>m33277 - Broken Hill</b>			<b>m39445 - Pachapaqui</b>			<b>m40106 - Franklin</b>		
<b>Center</b>	<b>FWHM</b>	<b>Area</b>	<b>Center</b>	<b>FWHM</b>	<b>Area</b>	<b>Center</b>	<b>FWHM</b>	<b>Area</b>
			<b>4145.6</b>	28.6	0.013			
			<b>3834.8</b>	32.7	0.002			
			<b>3536.1</b>	27.5	0.002			
			<b>3348.1</b>	19.8	0.004			
			<b>3198.1</b>	25.3	0.001			
						<b>1619.8</b>	4.3	0.003
			<b>1321.5</b>	54.1	0.008			
<b>1051.9</b>	9.8	0.040	<b>1051.4</b>	8.7	0.003	<b>1050.1</b>	8.0	0.002
						<b>1044.8</b>	13.7	0.029
			<b>1025.5</b>	7.4	0.002	<b>1030.1</b>	27.0	0.041
<b>1011.4</b>	35.7	0.080	<b>1005.2</b>	47.0	0.137	<b>1009.6</b>	17.6	0.040
<b>999.1</b>	13.6	0.179	<b>1000.3</b>	12.2	0.112	<b>1003.0</b>	13.5	0.097
<b>988.9</b>	13.5	0.064	<b>988.7</b>	14.0	0.081	<b>989.3</b>	15.0	0.055
<b>974.2</b>	12.1	0.073	<b>973.7</b>	10.3	0.061	<b>974.3</b>	12.1	0.085
<b>936.2</b>	10.4	0.016	<b>938.1</b>	9.7	0.009	<b>938.3</b>	10.5	0.017
<b>915.8</b>	21.1	0.006	<b>913.2</b>	17.9	0.007	<b>916.1</b>	18.7	0.008
						<b>887.2</b>	23.3	0.007
<b>878.7</b>	19.9	0.003	<b>877.6</b>	4.4	0.001	<b>877.3</b>	15.9	0.019
						<b>866.5</b>	2.9	0.002
<b>737.3</b>	13.8	0.005	<b>737.3</b>	10.2	0.008	<b>742.4</b>	14.0	0.004
<b>714.9</b>	11.8	0.012	<b>714.7</b>	16.2	0.018	<b>715.8</b>	20.3	0.005
<b>680.4</b>	7.3	0.006	<b>679.7</b>	8.3	0.012	<b>680.6</b>	9.9	0.014
						<b>670.0</b>	12.6	0.198
<b>667.3</b>	11.7	0.230	<b>667.5</b>	11.7	0.236	<b>664.6</b>	11.0	0.018
			<b>659.4</b>	8.8	0.017			
			<b>617.1</b>	23.9	0.003			
<b>570.7</b>	11.1	0.005	<b>572.3</b>	9.7	0.005	<b>572.2</b>	12.6	0.003
<b>556.2</b>	8.8	0.003	<b>557.1</b>	10.3	0.005	<b>558.2</b>	9.2	0.002
<b>542.9</b>	9.9	0.005	<b>543.6</b>	7.4	0.004	<b>546.8</b>	11.3	0.002
<b>513.2</b>	14.5	0.006	<b>509.5</b>	6.6	0.001	<b>512.6</b>	14.8	0.014
<b>495.2</b>	12.7	0.008	<b>496.8</b>	10.9	0.001	<b>494.9</b>	9.9	0.003
<b>473.7</b>	11.0	0.003	<b>473.0</b>	11.0	0.004			
<b>455.1</b>	16.4	0.010	<b>457.4</b>	21.2	0.005	<b>455.5</b>	19.1	0.008
<b>435.7</b>	12.7	0.014	<b>436.9</b>	11.9	0.013	<b>439.0</b>	8.3	0.002
						<b>421.9</b>	13.4	0.076
<b>416.2</b>	14.7	0.008	<b>413.6</b>	16.7	0.007	<b>409.1</b>	9.5	0.004
<b>390.5</b>	7.7	0.004	<b>388.9</b>	12.2	0.011	<b>391.2</b>	13.6	0.007
<b>386.1</b>	10.8	0.007						
<b>360.2</b>	19.4	0.034	<b>365.2</b>	27.1	0.014	<b>365.7</b>	13.4	0.007
<b>346.5</b>	11.1	0.009				<b>348.9</b>	7.8	0.003
						<b>343.1</b>	46.8	0.066
<b>337.3</b>	12.3	0.024	<b>336.5</b>	16.2	0.034	<b>335.5</b>	15.1	0.025
<b>321.1</b>	15.3	0.026	<b>322.9</b>	13.0	0.036	<b>324.8</b>	11.8	0.009
<b>298.5</b>	14.4	0.025	<b>298.9</b>	21.9	0.021			
			<b>292.0</b>	5.6	0.001			
<b>277.5</b>	15.2	0.015	<b>277.9</b>	14.4	0.015	<b>281.6</b>	17.4	0.002
<b>263.4</b>	10.4	0.016	<b>263.1</b>	12.8	0.023	<b>263.4</b>	7.9	0.003
						<b>259.1</b>	48.6	0.051
<b>247.6</b>	23.2	0.024	<b>244.5</b>	29.1	0.009	<b>246.7</b>	12.6	0.008

<b>217.6</b>	17.5	0.007	<b>225.1</b>	6.9	0.004			
<b>190.4</b>	19.0	0.003	<b>214.1</b>	11.5	0.010	<b>212.0</b>	17.2	0.006
<b>178.6</b>	7.4	0.002	<b>199.2</b>	6.8	0.000	<b>193.3</b>	11.2	0.004
<b>169.2</b>	9.3	0.002	<b>179.2</b>	5.5	0.002	<b>179.0</b>	6.4	0.001
<b>157.8</b>	9.2	0.002				<b>172.9</b>	27.2	0.006
<b>138.4</b>	13.2	0.001	<b>157.5</b>	4.5	0.001	<b>156.6</b>	7.2	0.001
						<b>135.3</b>	7.7	0.000

## **List of Figures**

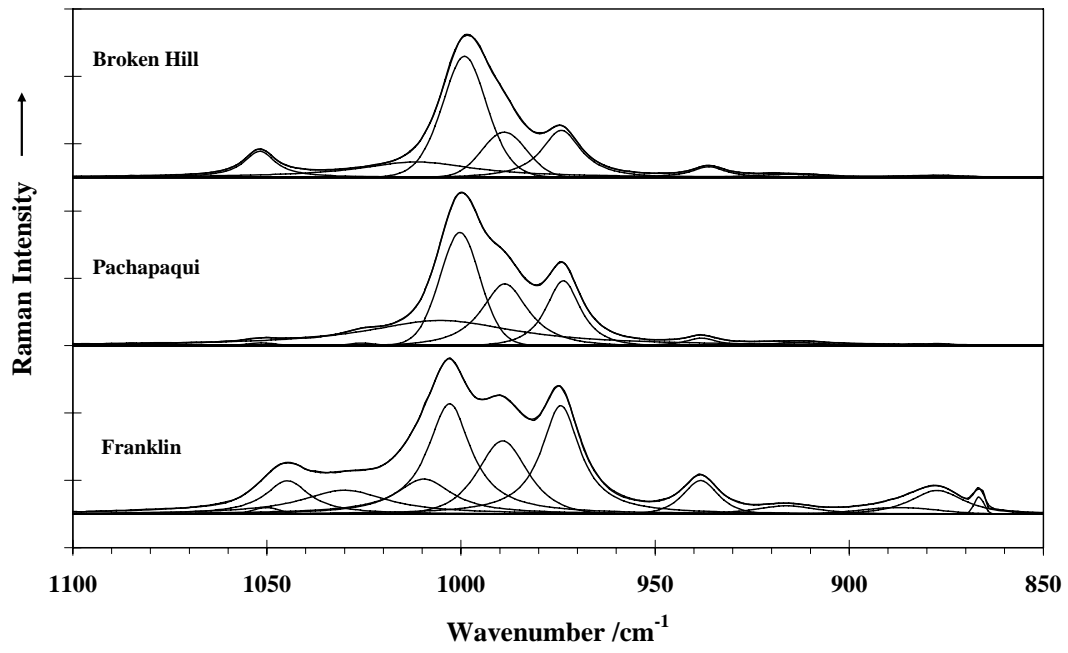
Figure 1 Raman spectra of the 850 to 1100  $\text{cm}^{-1}$  region of rhodonite from (a) Broken Hill (b) Pachapaquir (c) Franklin

Figure 2 Raman spectra of the 600 to 800  $\text{cm}^{-1}$  region of rhodonite from (a) Broken Hill (b) Pachapaquir (c) Franklin

Figure 3 Raman spectra of the 100 to 500  $\text{cm}^{-1}$  region of rhodonite from (a) Broken Hill (b) Pachapaquir (c) Franklin

## **List of Tables**

Table 1 Results of the Raman spectra of rhodonite



**Figure 1**

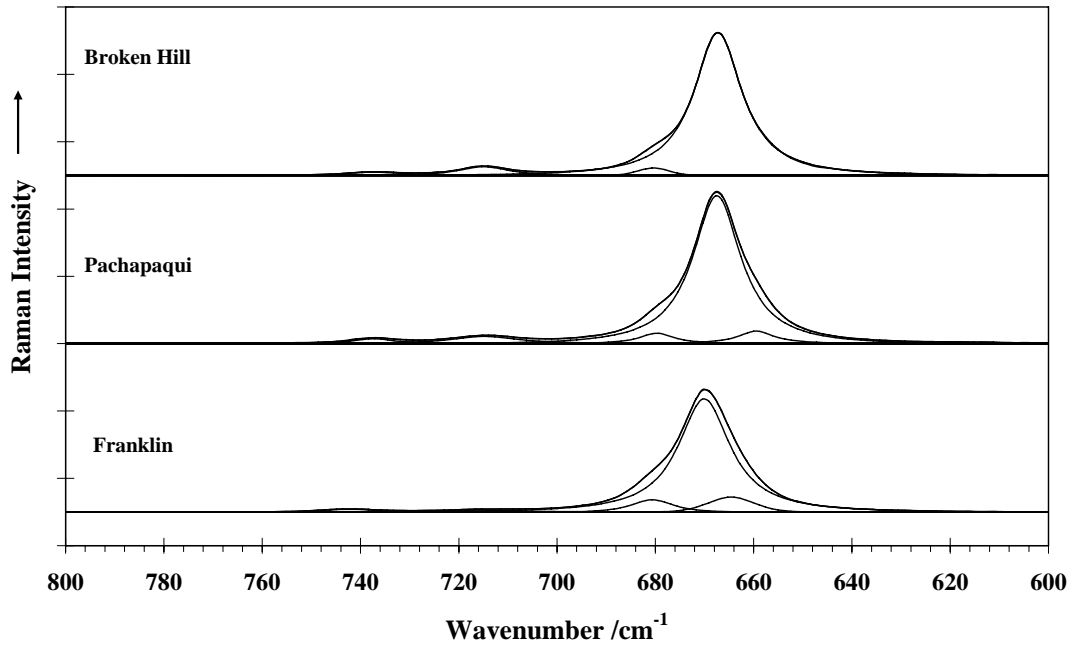


**Figure 2**

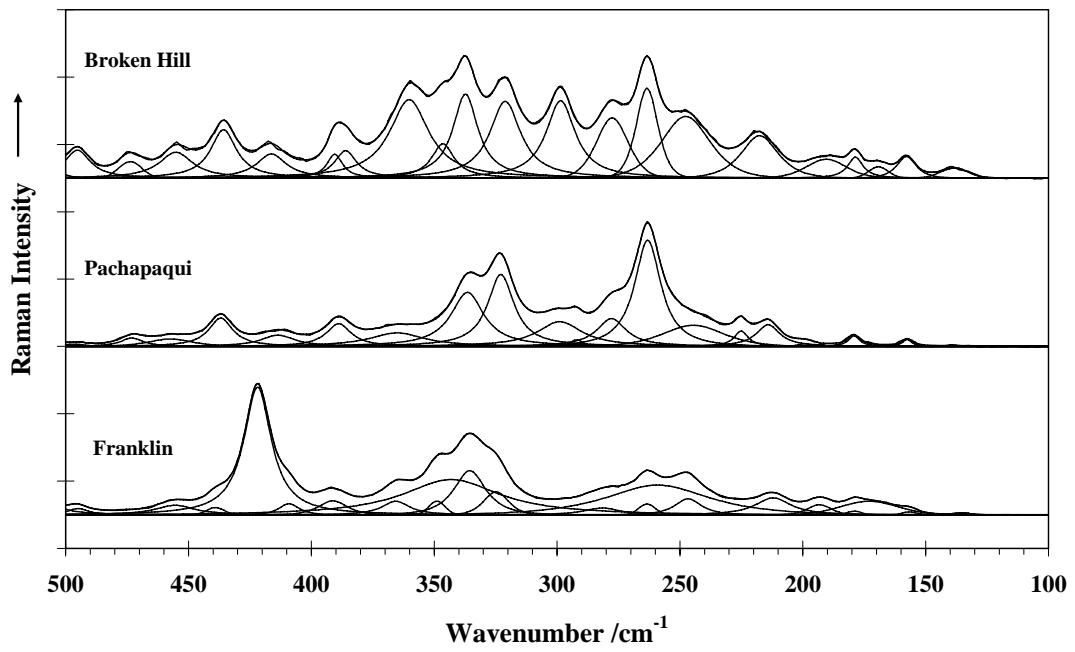


**Figure 3**